Carbohydrate Polymers 115 (2015) 575–581

Contents lists available at ScienceDirect

Carbohydrate Polymers

journal homepage: www.elsevier.com/locate/carbpol

Development of thermoplastic starch blown film by incorporating plasticized chitosan

Khanh Minh Dang [a], Rangrong Yoksan [a,b,*]

[a] Department of Packaging and Materials Technology, Faculty of Agro-Industry, Kasetsart University, Bangkok 10900, Thailand
[b] Center for Advanced Studies for Agriculture and Food, Kasetsart University, Bangkok 10900, Thailand

ARTICLE INFO

Article history:
Received 29 July 2014
Received in revised form 2 September 2014
Accepted 4 September 2014
Available online 16 September 2014

Keywords:
Thermoplastic starch
Chitosan
Extrusion
Blown film extrusion
Biodegradable film
Bio-based material

ABSTRACT

The objective of the present work was to improve blown film extrusion processability and properties of thermoplastic starch (TPS) film by incorporating plasticized chitosan, with a content of 0.37–1.45%. The effects of chitosan on extrusion processability and melt flow ability of TPS, as well as that on appearance, optical properties, thermal properties, viscoelastic properties and tensile properties of the films were investigated. The possible interactions between chitosan and starch molecules were evaluated by FTIR and XRD techniques. Chitosan and starch molecules could interact via hydrogen bonds, as confirmed from the blue shift of OH bands and the reduction of V-type crystal formation. Although the incorporation of chitosan caused decreased extensibility and melt flow ability, as well as increased yellowness and opacity, the films possessed better extrusion processability, increased tensile strength, rigidity, thermal stability and UV absorption, as well as reduced water absorption and surface stickiness. The obtained TPS/chitosan-based films offer real potential application in the food industry, e.g. as edible films.

1. Introduction

In recent decades, growing environmental consciousness has encouraged the development of biodegradable materials from renewable resources. Among plant-derived materials, starch offers several advantages as a raw material for the plastic industry, including its low cost, non-toxicity, biodegradability, compostability, and worldwide availability. Starch granules have been used as a plastic additive, e.g. as reinforcing agent and filler, for many years (Evangelista, Sung, Jane, Gelina, & Nikolov, 1991; Westhoff, Otey, Mehltretter, & Russell, 1974); however, only a small amount of starch could be added without the deterioration of plastic properties. In addition, starch has been transformed into thermoplastic material by applying heat and shear forces together with the incorporation of plasticizers (van Soest, Hulleman, de Wit, & Vliegenthart, 1996; Yu, Gao, & Lin, 1996). Although the resulting thermoplastic starch (TPS) can be converted into rigid or flexible packaging using conventional machines as for commodity plastics, its applications are limited due to high moisture absorption which causes surface stickiness (Thunwall, Kuthanova, Boldizar, & Rigdahl, 2008) as well as poor mechanical and barrier properties (Gáspár, Benkő, Dogossy, Réczey, & Czigány, 2005; Ma, Yu, & Kennedy, 2005; Pelissari et al., 2012; Yu, Prashantha, Soulestin, Lacrampe, & Krawczak, 2013). Blending/mixing TPS with other bio-based polymers such as chitosan (Pelissari, Grossmann, Yamashita, & Pineda, 2009; Pelissari, Yamashita, & Grossmann, 2011; Pelissari et al., 2012), cellulose (Gáspár et al., 2005; Ma et al., 2005), proteins (Gáspár et al., 2005), etc., has been reported to be a good technique for achieving fully bio-based materials and to widen the application window of TPS.

Chitosan, the linear cationic (1-4)-2-amino-2-deoxy-β-D-glucan is industrially produced from marine chitin ((1-4)-2-acetamido-2-deoxy-β-D-glucan) (Muzzarelli, 2012; Muzzarelli et al., 2012). Both of them have attracted attention owing to their superior characteristic properties, among which biocompatibility and absence of allergenicity (Busilacchi, Gigante, Mattioli-Belmonte, & Muzzarelli, 2013; Muzzarelli, 2009, 2010). Chitosan is a non-toxic (Kean & Thanou, 2010) and biodegradable (Bagheri-Khoulenjani, Taghizadeh, & Mirzadeh, 2009) polymer with antimicrobial activity (Cruz-Romero, Murphy, Morris, Cummins, & Kerry, 2013), all of which are important qualities for food packaging purposes. In general, chitosan is insoluble in water, alkali and most common organic solvents, but soluble in aqueous solutions of most organic acids, particularly lactic acid, formic acid and acetic acid with pH less than 6.

* Corresponding author at: Kasetsart University, Faculty of Agro-Industry, Department of Packaging and Materials Technology, 50 Ngamwongwan Rd., Ladyao, Chatuchak, Bangkok 10900, Thailand. Tel.: +66 2 562 5097; fax: +66 2 562 5046.
E-mail addresses: rangrong.y@ku.ac.th, yyrangrong@yahoo.com (R. Yoksan).

http://dx.doi.org/10.1016/j.carbpol.2014.09.005
0144-8617/

Incorporating chitosan into starch-based film has been reported as an alternative to reduce water affinity and improve its mechanical properties, due to the formation of intermolecular hydrogen bonds between amino and hydroxyl groups of chitosan and hydroxyl groups of starch (Xu, Kim, Hanna, & Nag, 2005). However, most previous studies have involved starch/chitosan-based films prepared by a solution casting method, in which the procedure is easy but the scale-up from laboratory to industrial level might be difficult because it is a very time-consuming process. Blown film extrusion is an alternative option to achieve industrial-scale output; however, few research articles have reported the development of starch/chitosan-based film using this method. Pelissari et al. (2009) revealed that starch/chitosan blown film composed of 5% chitosan showed decreased rigidity and water vapor permeability (WVP) as compared with the control, while the thermal stability of the films did not change. The processing parameters, such as die temperature and screw speed, also affect the properties of starch/chitosan blown film (Pelissari et al., 2011). Blow-up ratio and WVP of the film increased, while its opacity, tensile strength and elongation at break decreased with increasing screw speed. Low die temperatures caused decreased tensile properties and reduced WVP of the films. This research group also reported that the presence of a higher relative concentration of chitosan favored the formation of more rigid and opaque and less permeable films (Pelissari et al., 2012). It should be noted that chitosan flakes could not be melted during extrusion (Bonilla, Fortunati, Vargas, Chiralt, & Kenny, 2013; Grande & Carvalho, 2011); hence, homogenous chitosan-based films were acquired only by solvent casting of chitosan from an aqueous organic acid solution (Chillo et al., 2008; Xu et al., 2005). Blown film extrusion of a bio-based material composed of TPS and plasticized chitosan, in which the plasticized chitosan is derived from the protonation in aqueous acetic acid of chitosan followed by the intervention by glycerol, has not yet been reported, although it would be expected for preparing the homogeneous film.

Therefore, the objective of the present work was to develop film from TPS/chitosan-based materials, in which the chitosan was plasticized prior to incorporation into TPS via blown film extrusion.

2. Materials and methods

2.1. Materials

Native cassava starch (Dragon Fish brand) with moisture content of 11% of total weight was purchased from Tong Chan Registered Ordinary Partnership (Thailand). Chitosan (deacetylation degree of 85% and molecular weight of 500 kDa) was supplied by Seafresh Chitosan (Lab) Co., Ltd. (Thailand). Acetic acid (99%) was a product of Merck (Germany). The glycerol used was a commercial grade product.

2.2. Preparation of thermoplastic starch/chitosan-based compound resins by extrusion

Chitosan solutions – 0.37, 0.73, 1.09 and 1.45% – were prepared by dissolving chitosan flakes in an aqueous acetic acid solution (1% v/v, 100 mL), using a magnetic stirrer at 550 rpm until dissolution was complete (typically about 48 h at room temperature). Glycerol (25%) and subsequently starch were added to chitosan solutions and thoroughly mixed by agitation at ambient temperature for 15 min. Each slurry was then poured into a 1.5-cm-high plastic tray and kept in a hot-air oven at 65 °C for 18 h. The resulting dry material, with a moisture content of approximately 20–22%, was ground into powder and then blended using a twin-screw extruder with an L/D ratio of 40 and a screw diameter of 20 mm (LTE-20-40; Labtech Engineering Co., Ltd., Thailand), and with a barrel temperature profile of 90/95/105/110/115/120/120/120/120/125 °C (from hopper to die) and a screw speed of 170 rpm. The extrudates were cut into 2-mm-long pellets with a pelletizer. Four formulations of thermoplastic starch/chitosan-based compound resins were obtained: i.e. TPS/CTS0.37, TPS/CTS0.73, TPS/CTS1.09 and TPS/CTS1.45, representing thermoplastic starch with a chitosan content of 0.37, 0.73, 1.09 and 1.45%, respectively. TPS without addition of chitosan was also prepared and used as a control.

2.3. Preparation of thermoplastic starch/chitosan-based films by blown film extrusion

The obtained resins were blown into films using a single-screw extruder (LE-25-30/C; Labtech Engineering) – with an L/D ratio of 30, a screw diameter of 25 mm, and four controlled temperature zones – connected to a film-blowing attachment (LF-400; Labtech Engineering) with a ring-shaped die. The barrel temperature profile was maintained at 130/140/140/140 °C (from feed inlet to die) and the die temperature was set at 150 °C. Screw speed and nip roll speed were adjusted to 35–45 rpm and 3 rpm, respectively.

2.4. Characterization and properties testing of thermoplastic starch/chitosan-based compound resins and films

2.4.1. Melt flow index measurement

Melt flow index (MFI) of the samples was measured according to ASTM 1238-10, with a slight modification. The measurement was performed using an MFI-2 (Custom Scientific Instruments, USA) at 190 °C with a load cell of 3.2 kg, a preheating time of 7 min and a time interval of 6 min. MFI was measured in triplicate for each sample and reported in g/10 min as mean ± SD ($n = 3$).

2.4.2. Color measurement

Color of the films was measured using a CR-400 colorimeter (Konica Minolta, Japan). The measurements were performed in triplicate in the CIE 1976 (L^*, a^*, b^*) color space (or CIELAB), where L^*, a^* and b^* indicate lightness, redness and yellowness, respectively.

2.4.3. Measurement of UV absorption and transparency

UV absorption and light transmittance of the films were measured at wavelength ranges of 200 nm to 400 nm and 400 nm to 800 nm, respectively, using a UV-2450 Ultraviolet–visible (UV–vis) spectrophotometer (Shimadzu, Japan).

2.4.4. Fourier transform infrared analysis

Fourier transform infrared (FT-IR) spectra of the samples were recorded in attenuated total reflectance (ATR) mode using a Bruker Tensor 27 FT-IR spectrometer (Bruker, Germany). The spectra were recorded at a wavenumber range from 500 cm^{-1} to 4000 cm^{-1} at temperatures varying from 30 °C to 220 °C, using 32 accumulated scans and a spectral resolution of 4 cm^{-1}.

2.4.5. X-ray diffraction analysis

X-ray diffraction (XRD) patterns of the samples were analyzed by a JEOL JDX-3530 X-ray diffractomer (JEOL, Japan). Samples were scanned at diffraction angles (2θ) from 5 to 40° using a scan rate of 0.02°/s.

2.4.6. Thermogravimetric analysis

TGA thermograms were obtained using a STA PT1000 TG-DSC (Linseis, Germany) with TA evaluation software. Each sample (15–25 mg) was placed in a ceramic crucible and heated from 25 °C to 600 °C at a heating rate of 20 °C/min under a nitrogen atmosphere with a N_2 flow rate of 4 L/h.

Table 1
Extrusion parameters for TPS and TPS/CTS compounds and films.

Sample	Compounding extrusion[a]			Blown film extrusion[b]	
	Pressure (bar)	Torque (%)	Output rate (kg/h)	Pressure (bar)	Torque (%)
TPS	24–35	53–54	0.44 ± 0.034	121–135	61–71
TPS/CTS0.37	35–45	53–54	0.62 ± 0.028	168–183	67–77
TPS/CTS0.73	39–51	53–54	0.62 ± 0.036	175–191	70–80
TPS/CTS1.09	48–60	53–54	0.94 ± 0.035	188–203	73–89
TPS/CTS1.45	53–65	53–54	1.19 ± 0.035	190–204	71–89

[a] Using a barrel temperature profile of 90/95/105/110/115/120/120/120/120/125 °C (from hopper to die) and a screw speed of 170 rpm.
[b] Using a barrel temperature profile of 130/140/140/140 °C (from feed inlet to die), a die temperature of 150 °C, a screw speed of 35–45 rpm and a nip roll speed of 3 rpm.

2.4.7. Dynamic mechanical thermal analysis

Dynamic mechanical thermal analysis (DMTA) was performed with an EPLEXOR® DMA (GABO Qualimeter, Germany) in a tension mode at a frequency of 1.5 Hz, a static load of 0.5 N and a dynamic load of 0.15 N. Scanning temperature was from −80 °C to 55 °C with a heating rate of 3 °C/min. Each sample was cut into a rectangular shape with a dimension of 10 mm × 50 mm. Grips were used to hold the sample firmly without causing excessive deformation before testing. Storage modulus (E') and tan delta ($\tan\delta$) were evaluated. Three replications were performed for each sample.

2.4.8. Tensile testing

Tensile properties of the film samples were tested using a 5965 universal testing machine (Instron, USA) according to ASTM standard method D882-12 (2012) with modified storage conditions. Samples were cut into rectangular shapes with a dimension of 3 cm × 15 cm and then conditioned at ambient temperature with different relative humidity (RH) of 62 ± 2% and 42 ± 2% for at least two days prior to the test. Five specimens were tested for each sample. Thickness of the films was measured by an ID-C112BS micrometer (Mitutoyo, Japan), with an accuracy of 0.0001 mm. The average thickness of each film was calculated from five points for each specimen. Tensile strength (MPa), modulus of elasticity (MPa) and elongation at break (%) were recorded as mean ± SD (n = 5). The initial grip distance was set at 100 mm and the crosshead speed was 50 mm/min.

3. Results and discussion

3.1. Extrusion processability and melt flow ability of thermoplastic starch/chitosan-based compounds

Table 1 shows the processing parameters, i.e. induced pressure and torque as well as the output rate, for compounding extrusion and blown film extrusion of TPS and TPS/CTS materials. For films produced by the compounding process using a twin-screw extruder, TPS possessed induced pressure of 24–35 bar, while TPS/CTS compounds exhibited higher induced pressure, in the range of 35–65 bar. The induced pressure of the TPS/CTS compounds increased with increasing chitosan concentration, implying that the material became viscous, probably due to the interaction or entanglement between starch and chitosan molecules. Although the induced pressure became higher as chitosan content increased, extrusion of the TPS/CTS compounds could be performed without any difficulty as the torque of the system remained essentially unchanged. In addition, the increased induced pressure provided not only easier processing but also a greater output rate of the products (Table 1). The output rate of TPS/CTS compounds was almost twice as high as that of TPS when 1.45% of chitosan was incorporated.

Similarly, TPS/CTS compounds also exhibited higher induced pressure during blown film extrusion (168–204 bar) compared with TPS (121–135 bar) (Table 1), corresponding to the higher blown film production rate (data not shown). The torque of the system tended to increase with increasing chitosan concentration due to the increased melt viscosity or decreased flow ability. It should be pointed out that although both TPS and TPS/CTS compounds could be continuously blown into films (Fig. 1A), the obtained TPS/CTS films possessed tunable thickness due to their higher melt strength. In addition, the TPS/CTS films had reduced surface stickiness and greater opacity (Fig. 1Ab) as compared with TPS film (Fig. 1Aa).

Melt flow behavior of TPS and TPS/CTS compounds was evaluated from the melt flow index (MFI), measured at 190 °C with a load cell of 3.2 kg. MFI value of TPS was about 1.32 g/10 min, while those of TPS/CTS compounds varied from 0.09 g/10 min to 0.81 g/10 min (Fig. 1B). The results showed that the melt flow ability of TPS decreased, or its melt viscosity increased, by incorporating chitosan. In addition, the melt flow ability significantly decreased with increasing chitosan content: for example, by almost three times for TPS/CTS0.73 as compared with TPS/CTS0.37. The reduction of melt flow ability might result from the interaction between starch and chitosan molecules.

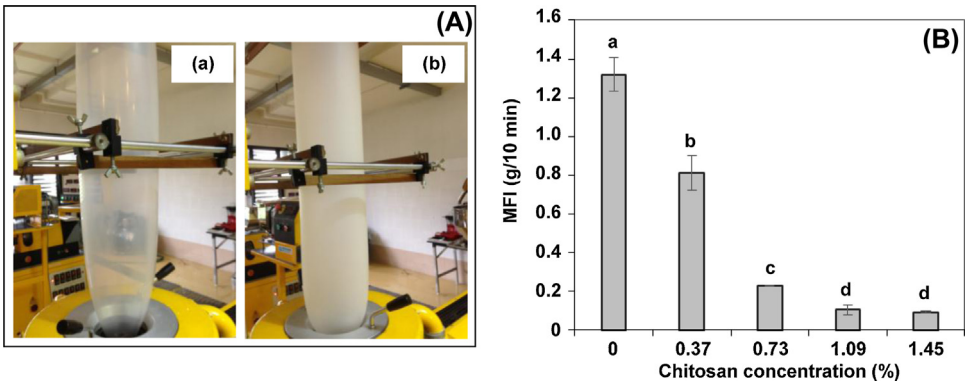

Fig. 1. (A) Blown film extrusion of (a) TPS and (b) TPS/CTS1.45 and (B) melt flow index of TPS and TPS/CTS compounds containing different chitosan concentrations. Data are reported as mean ± SD, n = 3. Different lower-case letters indicate a significant difference at $p < 0.05$ (Duncan's new multiple range test).

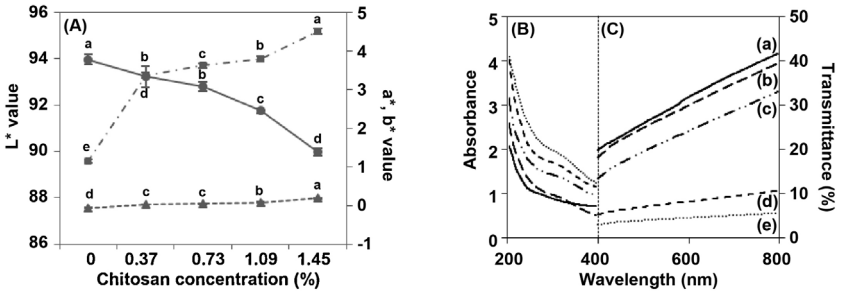

Fig. 2. (A) Color parameters: L^* (●), a^* (▲) and b^* (■), (B) UV absorbance and (C) light transmittance of different film samples: (a) TPS, (b) TPS/CTS0.37, (c) TPS/CTS0.73, (d) TPS/CTS1.09 and (e) TPS/CTS1.45. For (A), data are reported as mean ± SD, $n = 3$. Different lower-case letters indicate a significant difference at $p < 0.05$ (Duncan's new multiple range test).

3.2. Color, transparency and UV absorption of thermoplastic starch/chitosan-based films

Color and transparency of packaging films are important in terms of general appearance, consumer acceptance and utilization. Fig. 2A shows that L^* values of TPS/CTS films were lower than that of TPS film; also, the L^* values of TPS/CTS films significantly decreased with increasing chitosan concentration. This result implied that the presence of chitosan caused a darker film. TPS film showed slightly increased a^* value and markedly increased b^* value when chitosan was incorporated. However, the film color was still a red/yellow shade, since a^* and b^* values were positive. The values of a^* and b^* of TPS/CTS films tended to increase with increasing chitosan content; this was reflected by the films becoming a darker yellow.

UV absorption of the films was measured at a wavelength range from 200 nm to 400 nm. TPS/CTS films showed higher UV absorption than TPS film, and UV absorption of the TPS/CTS films increased with increasing chitosan content (Fig. 2B). The result suggested that chitosan could impart UV light protection to TPS film; this might be useful for retarding lipid oxidation induced by UV light. Bonilla et al. (2013) also reported that PLA/CTS films showed better barrier properties against UV light than naked PLA film.

Transparency of the films was determined from light transmission at selected wavelengths from 400 nm to 800 nm. The transmittance values of all samples increased with increasing wavelength (Fig. 2C). TPS/CTS films showed lower light transmittance values than TPS film, corresponding to the abovementioned opacity (Fig. 1A). Higher chitosan contents gave the films greater opacity, due to the highly dispersed chitosan in the TPS/CTS matrix.

3.3. Chemical interaction of thermoplastic starch/chitosan-based films

FITR spectroscopy was applied to examine the chemical interaction between starch and chitosan. TPS film exhibited characteristic bands at 3283 cm^{-1} (O—H stretching), 2928 cm^{-1} (C—H stretching), 1640 cm^{-1} (δ(O—H) bending of water), 1365 cm^{-1} (CH_2), 1015 cm^{-1} (C—O—C bond stretching) and 926 cm^{-1} (pyranose ring) (Delval et al., 2004) (Fig. 3Aa). All TPS/CTS films showed similar FTIR spectra (Fig. 3Ab–e) to that of TPS film; because a relatively tiny

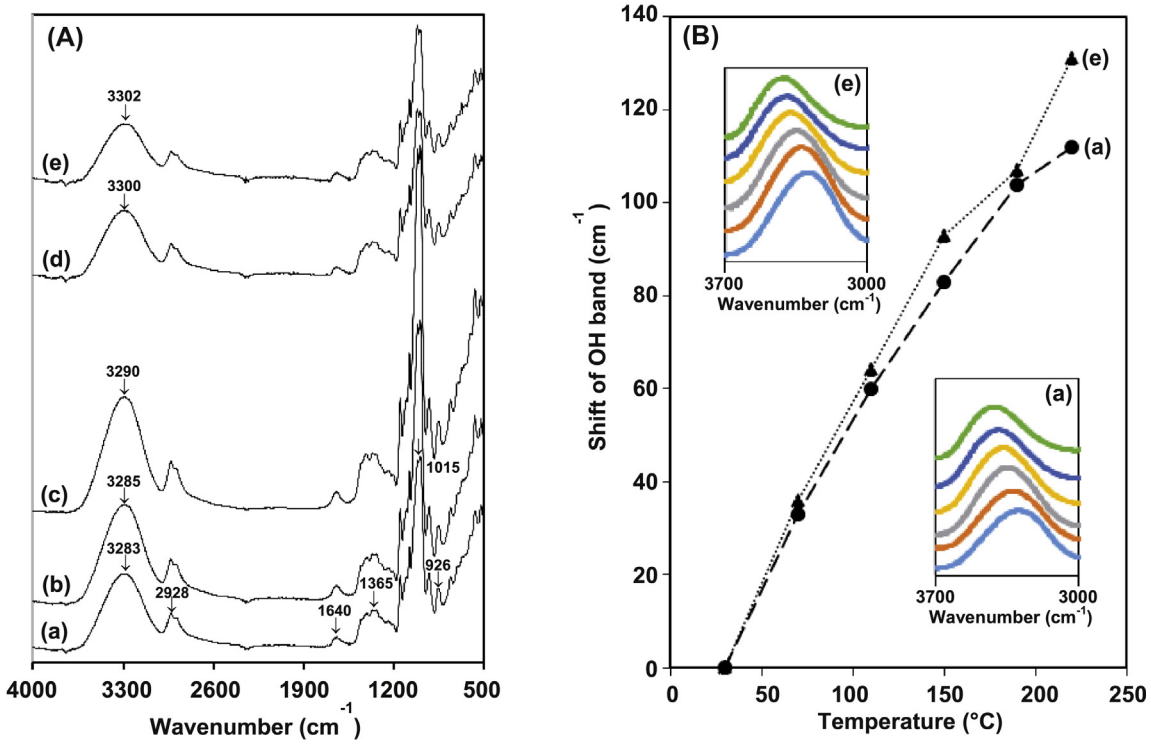

Fig. 3. (A) FTIR spectra and (B) shift of the OH band of different film samples: (a) TPS, (b) TPS/CTS0.37, (c) TPS/CTS0.73, (d) TPS/CTS1.09 and (e) TPS/CTS1.45. Inset of (B) represents FTIR spectra as a function of temperature: from bottom to top, 30 °C, 70 °C, 110 °C, 150 °C, 190 °C and 220 °C.

amount of chitosan was added, most of the characteristic peaks of chitosan appeared at the same positions as those of starch. Hydrogen bonding between starch and chitosan molecules was expected to be a possible interaction in the TPS/CTS system. Fig. 3A also shows that the OH band of starch was shifted to a higher wavenumber when chitosan was added, implying that hydrogen bonds between starch molecules became weaker because some of them formed intermolecular hydrogen bonds with chitosan. However, hydrogen bond interaction was difficult to evaluate from the spectra characterized at room temperature (60% RH) due to the effect of moisture. Skrovanek, Howe, Painter, and Coleman (1985) and Coleman and Painter (1990) reported that the destruction of hydrogen bonds could be observed at high temperature. Herein, FTIR spectra of the samples were analyzed at various temperatures from 30 °C to 220 °C. Fig. 3B shows that the OH bands of both TPS and TPS/CTS films became broader with lower intensity and shifted to higher frequency when temperature was increased, reflecting the reduction of the average strength of the hydrogen bonds and a broadening of the distribution (Eichhorn, Fahmi, Adam, & Stamm, 2003; Kössler, Chemie, & Věd, 1990). However, TPS/CTS film showed a higher degree of OH band shift than TPS film (Fig. 3B), indicating that hydrogen bonds between starch molecules became weaker when chitosan was incorporated because chitosan could form hydrogen bond interaction with starch molecules.

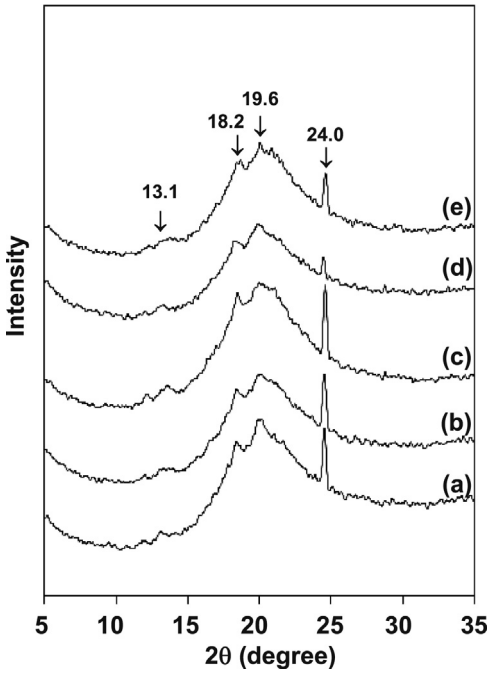

Fig. 4. XRD patterns of different film samples: (a) TPS, (b) TPS/CTS0.37, (c) TPS/CTS0.73, (d) TPS/CTS1.09 and (e) TPS/CTS1.45.

3.4. Crystal structure of starch in thermoplastic starch/chitosan-based films

The crystal type of starch in the film samples was analyzed by XRD technique. TPS film showed characteristic diffraction peaks at 2θ of 13.1°, 18.2°, 19.6° and 24.0° (Fig. 4a). The peaks at 2θ of 13.1° and 19.6° were ascribed to V_H-type crystals formed by complexation of amylose and glycerol (van Soest & Essers, 1997), whereas the peaks at 2θ of 18.2° and 24.0° belonged to B-type crystals (Myllärinen, Buleon, Lahtinen, & Forssell, 2002), which might form during storage. High water uptake of the material, as well as storage conditions of high relative humidity (e.g. >60% RH) and temperature (particularly higher than the glass transition temperature of the material), can speed up B-type crystal formation due to the high mobility of starch molecular chains. Rindlav-Westling, Stading, Hermansson, and Gatenholm (1998) disclosed that increased air humidity during film formation led to a longer contact time with water, resulting in high mobility of the starch polymeric chains and subsequently increased B-type crystallinity. V-type crystal bands became broader with increasing chitosan content; this implied that the number of amylose–glycerol complexes decreased due to limited amylose mobility, since it formed hydrogen bond interaction with chitosan. Zhong, Song, and Li (2011) also found that kudzu starch–chitosan composite films showed broad amorphous peaks as compared with starch film, demonstrating that the intermolecular interactions among the components limited the movements of molecular chain segments and restrained the crystallization process.

3.5. Thermal stability of thermoplastic starch/chitosan-based films

Thermal stability of TPS and TPS/CTS films was evaluated by TGA technique. TPS film clearly illustrated a three-step weight loss at temperature ranges of 80–106 °C, 106–200 °C and 200–360 °C, attributed to free water evaporation (Pelissari et al., 2009), bound water and glycerol evaporation (Cyras, Manfredi, Ton-That, & Vázquez, 2008), and starch decomposition (Pelissari et al., 2009), respectively (Fig. 5Aa). However, TPS/CTS films exhibited two-step weight loss at temperature ranges of 80–240 °C and 240–360 °C, ascribed to water and glycerol evaporation (Cyras et al., 2008) and decomposition of starch and chitosan (Pelissari et al., 2009), respectively (Fig. 5Ab–e). The weight reduction of the film decreased when chitosan was incorporated, and it also decreased with increasing chitosan content. For example, total weight loss of TPS film at 250 °C was 20.9%, while those of TPS/CTS films were in the range of 10.6–15.9%. After decomposition at 350 °C, the remaining weight of TPS film was lowest while those of TPS/CTS films were higher, implying that TPS/CTS films contained a larger amount of inorganic

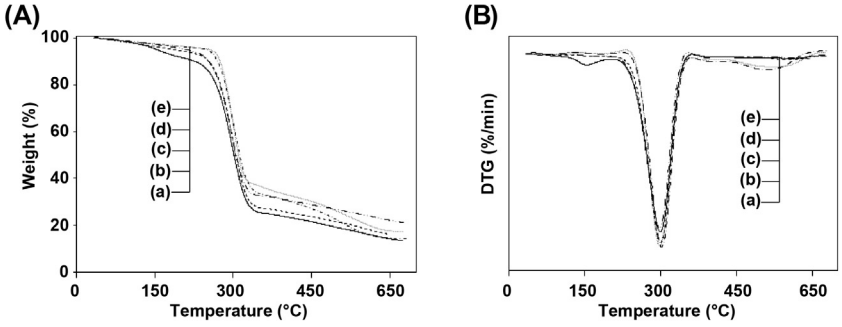

Fig. 5. (A) TGA and (B) DTG thermograms of different film samples: (a) TPS, (b) TPS/CTS0.37, (c) TPS/CTS0.73, (d) TPS/CTS1.09 and (e) TPS/CTS1.45.

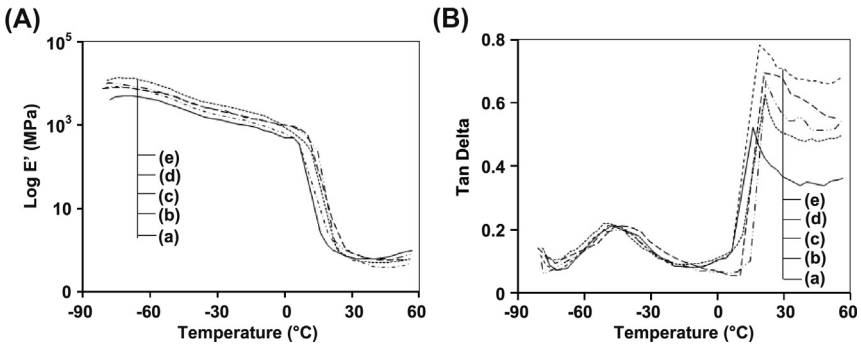

Fig. 6. (A) Storage modulus and (B) tan δ of different film samples: (a) TPS, (b) TPS/CTS0.37, (c) TPS/CTS0.73, (d) TPS/CTS1.09 and (e) TPS/CTS1.45.

substances. The above results indicated that TPS film became less hygroscopic and more thermally stable when chitosan was incorporated. This might be due to hydrogen bond formation between the two polymers. However, the decomposition temperature (T_d) of TPS film hardly changed with the addition of chitosan, i.e. ~300 °C (Fig. 5B).

3.6. Dynamic mechanical thermal properties of thermoplastic starch/chitosan-based films

Viscoelastic or phase relaxation behavior of TPS and TPS/CTS films was studied by DMTA technique at a frequency of 1.5 Hz, a static load of 0.5 N and a dynamic load of 0.15 N. The storage modulus (E') is generally relevant to the stored energy, representing the elastic portion of the material, while the loss modulus (E'') is used to indicate the energy dissipated as heat, representing the viscous portion. Tan δ (loss factor) is defined as the ratio of loss modulus to storage modulus ($\tan\delta = E''/E'$), where δ is the angle between in-phase and out-phase components of the modulus in the cyclic motion.

Storage modulus of all samples slightly decreased with increasing temperature up to 10 °C and then sharply decreased until 23 °C (Fig. 6A), implying that the materials became softer upon heating. The marked reduction of storage modulus of the latter involved the transition of the materials from glassy to rubbery states. At temperatures below the transition point, TPS/CTS films exhibited higher storage modulus than TPS film, and the storage modulus of the films increased with increasing chitosan content (Fig. 6A). This result indicated that incorporating chitosan enhanced the stiffness of the TPS film. This could be explained by the lower chain mobility of starch due to its interaction with chitosan.

Glass transition temperature (T_g) of the components in TPS and TPS/CTS films could be determined from the highest transition peak of the loss factor–temperature curve. Tan δ curves described a partially miscible system, with two main relaxations appearing at −50 °C to −40 °C and 16 °C to 22 °C, attributed to T_g of the glycerol-rich phase and T_g of starch in TPS, respectively (da Róz, Carvalho, Gandini, & Curvelo, 2006) (Fig. 6B). Starch in TPS film showed T_g of 16 °C, whereas starch in TPS/CTS films possessed T_g values in the range of 19.2–22.1 °C. The results showed that T_g of starch in TPS increased when chitosan was incorporated, indicating that the mobility of starch chains in the TPS/CTS films was restrained due to the interaction between starch and chitosan.

3.7. Tensile properties of thermoplastic starch/chitosan-based films

Tensile properties of TPS and TPS/CTS films were tested after conditioning at 42 ± 2% RH and 62 ± 2% RH. At 42 ± 2% RH, tensile strength (TS) and Young's modulus of TPS film increased, while its elongation at break decreased by incorporating chitosan with a content of 0.37–1.45% (Fig. 7). In addition, the augmentation of TS and Young's modulus, as well as the reduction of elongation at break, of TPS/CTS films increased with increasing chitosan content. The results suggested that the film became stronger, more rigid and less extensible when chitosan was loaded. This might be a result of the formation of intermolecular hydrogen bonds between starch and chitosan molecules. Pelissari et al. (2012) and Xu et al. (2005) also reported that the tensile strength of cassava starch/chitosan films prepared by two different methods (i.e. blown film extrusion and solution casting) increased with increasing chitosan content, attributed to the formation of intermolecular hydrogen bonding between the —NH_2 groups present in the structure of chitosan and the —OH groups of cassava starch.

However, TS and Young's modulus of the films stored at 62 ± 2% RH increased slightly when chitosan was incorporated, while

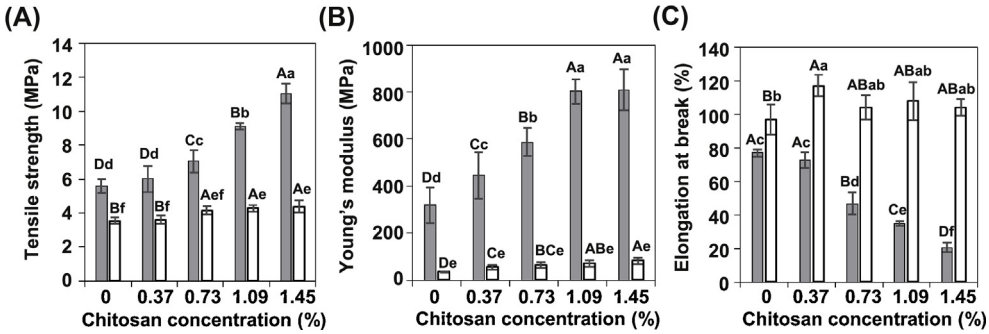

Fig. 7. (A) Tensile strength, (B) Young's modulus and (C) elongation at break of TPS and TPS/CTS films containing different chitosan concentrations after storage at 42 ± 2% RH (■) and 62 ± 2% RH (□). Data are reported as mean ± SD, $n = 5$. Different upper-case letters indicate a significant difference at $p < 0.05$ (Duncan's new multiple range test) of data for different chitosan concentrations, and different lower-case letters indicate a significant difference at $p < 0.05$ (Duncan's new multiple range test) of data for different sample storage conditions.

elongation at break hardly changed. It might be assumed that the effect of absorbed moisture/water, which could act as a plasticizer, was more predominant than the effect of chitosan. Perdomo et al. (2009) found that water could plasticize cassava starch at high moisture content, resulting in decreased T_g, which in turn softens the material.

TPS and TPS/CTS films conditioned at 62 ± 2% RH showed lower TS and Young's modulus but higher elongation at break than those conditioned at 42 ± 2% RH, reflecting that the films lost their strength and became more flexible when they were stored under conditions of higher relative humidity. This might be explained by the plasticizing effect of moisture absorbed by the samples. The above results also suggest that the relative humidity of the environment or the moisture content of the samples strongly affected the tensile properties of the TPS-based films.

4. Conclusion

TPS/CTS based materials were prepared using a twin-screw extruder and then converted into a film by blown film extrusion. FTIR results showed that chitosan could form hydrogen bond interaction with starch, resulting in decreased V-type crystallinity and positive effects on film properties. The addition of 0.37–1.45% of chitosan improved strength (tensile strength increased ~8–97%), stiffness (Young's modulus increased ~40–154%), and thermal stability as well as reduced water absorption of the TPS film. However, extensibility of TPS film decreased (elongation at break decreased ~5–73%) when chitosan was incorporated. Compared with TPS film, TPS/CTS films were a more intense yellow with increased opacity, and also showed greater UV absorption.

Acknowledgements

The authors are grateful for financial support from: the Kasetsart University Research and Development Institute, Thailand (Grant No. SRU 3.55); the Commission on Higher Education, Ministry of Education, Thailand (National Research University of Thailand); and the Faculty of Agro-Industry, Kasetsart University, Thailand (through the Scholarships for International Graduate Students 2012).

References

Bagheri-Khoulenjani, S., Taghizadeh, S. M., & Mirzadeh, H. (2009). An investigation on the short-term biodegradability of chitosan with various molecular weights and degrees of deacetylation. *Carbohydrate Polymers*, *78*(4), 773–778.

Bonilla, J., Fortunati, E., Vargas, M., Chiralt, A., & Kenny, J. M. (2013). Effects of chitosan on the physicochemical and antimicrobial properties of PLA films. *Journal of Food Engineering*, *119*(2), 236–243.

Busilacchi, A., Gigante, A., Mattioli-Belmonte, M., & Muzzarelli, R. A. A. (2013). Chitosan stabilizes platelet growth factors and modulates stem cell differentiation toward tissue regeneration. *Carbohydrate Polymers*, *98*, 665–676.

Chillo, S., Flores, S., Mastromatteo, M., Conte, A., Gerschenson, L., & Del Nobile, M. A. (2008). Influence of glycerol and chitosan on tapioca starch-based edible film properties. *Journal of Food Engineering*, *88*(2), 159–168.

Coleman, M. M., & Painter, P. C. (1990). Infrared-absorption spectroscopy. In J. I. Kroschwitz (Ed.), *Polymers: Polymer characterization and analysis* (pp. 371–403). New York, NY: John Wiley & Sons.

Cruz-Romero, M. C., Murphy, T., Morris, M., Cummins, E., & Kerry, J. P. (2013). Antimicrobial activity of chitosan, organic acids and nano-sized solubilisates for potential use in smart antimicrobially-active packaging for potential food applications. *Food Control*, *34*(2), 393–397.

Cyras, V. P., Manfredi, L. B., Ton-That, M.-T., & Vázquez, A. (2008). Physical and mechanical properties of thermoplastic starch/montmorillonite nanocomposite films. *Carbohydrate Polymers*, *73*(1), 55–63.

da Róz, A., Carvalho, A. J. F., Gandini, A., & Curvelo, A. A. S. (2006). The effect of plasticizers on thermoplastic starch compositions obtained by melt processing. *Carbohydrate Polymers*, *63*(3), 417–424.

Delval, F., Crini, G., Bertini, S., Morin-Crini, N., Badot, P.-M., Vebrel, J., et al. (2004). Characterization of crosslinked starch materials with spectroscopic techniques. *Journal of Applied Polymer Science*, *93*(6), 2650–2663.

Eichhorn, K.-J., Fahmi, A., Adam, G., & Stamm, M. (2003). Temperature-dependent FTIR spectroscopic studies of hydrogen bonding of the copolymer poly(styrene-*b*-4-vinylpyridine) with pentadecylphenol. *Journal of Molecular Structure*, *661–662*, 161–170.

Evangelista, R. L., Sung, W., Jane, J. L., Gelina, R. J., & Nikolov, Z. L. (1991). Effect of compounding and starch modification on properties of starch-filled low-density polyethylene. *Industrial & Engineering Chemistry Research*, *30*(8), 1841–1846.

Gáspár, M., Benkő, Z., Dogossy, G., Réczey, K., & Czigány, T. (2005). Reducing water absorption in compostable starch-based plastics. *Polymer Degradation and Stability*, *90*(3), 563–569.

Grande, R., & Carvalho, A. J. (2011). Compatible ternary blends of chitosan/poly(vinyl alcohol)/poly(lactic acid) produced by oil-in-water emulsion processing. *Biomacromolecules*, *12*(4), 907–914.

Kean, T., & Thanou, M. (2010). Biodegradation, biodistribution and toxicity of chitosan. *Advanced Drug Delivery Reviews*, *62*(1), 3–11.

Ma, X., Yu, J., & Kennedy, J. F. (2005). Studies on the properties of natural fibers-reinforced thermoplastic starch composites. *Carbohydrate Polymers*, *62*(1), 19–24.

Muzzarelli, R. A. A. (2009). Chitins and chitosans for the repair of wounded skin, nerve, cartilage and bone. *Carbohydrate Polymers*, *76*, 167–182.

Muzzarelli, R. A. A. (2010). Chitins and chitosans as immunoadjuvants and non-allergenic drug carriers. *Marine Drugs*, *8*(2), 292–312.

Muzzarelli, R. A. A. (2012). Nanochitins and nanochitosans, paving the way to eco-friendly and energy-saving exploitation of marine resources. *Polymer Science: A Comprehensive Reference*, *10*, 153–164.

Muzzarelli, R. A. A., Boudrant, J., Meyer, D., Manno, N., DeMarchis, M., & Paoletti, M. G. (2012). A tribute to Henri Braconnot, precursor of the carbohydrate polymers science, on the chitin bicentennial. *Carbohydrate Polymers*, *87*, 995–1012.

Myllärinen, P., Buleon, A., Lahtinen, R., & Forssell, P. (2002). The crystallinity of amylose and amylopectin films. *Carbohydrate Polymers*, *48*(1), 41–48.

Pelissari, F. M., Grossmann, M. V., Yamashita, F., & Pineda, E. A. (2009). Antimicrobial, mechanical, and barrier properties of cassava starch–chitosan films incorporated with oregano essential oil. *Journal of Agricultural and Food Chemistry*, *57*(16), 7499–7504.

Pelissari, F. M., Yamashita, F., Garcia, M. A., Martino, M. N., Zaritzky, N. E., & Grossmann, M. V. E. (2012). Constrained mixture design applied to the development of cassava starch–chitosan blown films. *Journal of Food Engineering*, *108*(2), 262–267.

Pelissari, F. M., Yamashita, F., & Grossmann, M. V. E. (2011). Extrusion parameters related to starch/chitosan active films properties. *International Journal of Food Science & Technology*, *46*(4), 702–710.

Perdomo, J., Cova, A., Sandoval, A. J., García, L., Laredo, E., & Müller, A. J. (2009). Glass transition temperatures and water sorption isotherms of cassava starch. *Carbohydrate Polymers*, *76*(2), 305–313.

Rindlav-Westling, A., Stading, M., Hermansson, A.-M., & Gatenholm, P. (1998). Structure, mechanical and barrier properties of amylose and amylopectin films. *Carbohydrate Polymers*, *36*(2–3), 217–224.

Skrovanek, D. J., Howe, S. E., Painter, P. C., & Coleman, M. M. (1985). Hydrogen bonding in polymers: Infrared temperature studies of an amorphous polyamide. *Macromolecules*, *18*(9), 1676–1683.

Thunwall, M., Kuthanova, V., Boldizar, A., & Rigdahl, M. (2008). Film blowing of thermoplastic starch. *Carbohydrate Polymers*, *71*(4), 583–590.

van Soest, J. J. G., Hulleman, S. H. D., de Wit, D., & Vliegenthart, J. F. G. (1996). Crystallinity in starch bioplastics. *Industrial Crops and Products*, *5*(1), 11–22.

van Soest, J. J. G., & Essers, P. (1997). Influence of amylose–amylopectin ratio on properties of extruded starch plastic sheets. *J. Macromol. Sci. A: Pure Appl. Chem.*, *34*(9), 1665–1689.

Westhoff, R. P., Otey, F. H., Mehltretter, C. L., & Russell, C. R. (1974). Starch-filled polyvinyl chloride plastics—Preparation and evaluation. *Industrial & Engineering Chemistry Product Research and Development*, *13*(2), 123–125.

Xu, Y. X., Kim, K. M., Hanna, M. A., & Nag, D. (2005). Chitosan–starch composite film: Preparation and characterization. *Industrial Crops and Products*, *21*(2), 185–192.

Yu, F., Prashantha, K., Soulestin, J., Lacrampe, M. F., & Krawczak, P. (2013). Plasticized-starch/poly(ethylene oxide) blends prepared by extrusion. *Carbohydrate Polymers*, *91*(1), 253–261.

Yu, J., Gao, J., & Lin, T. (1996). Biodegradable thermoplastic starch. *Journal of Applied Polymer Science*, *62*(9), 1491–1494.

Zhong, Y., Song, X., & Li, Y. (2011). Antimicrobial, physical and mechanical properties of kudzu starch–chitosan composite films as a function of acid solvent types. *Carbohydrate Polymers*, *84*(1), 335–342.